Frontiers in Bioscience Landmark

Front. Biosci. (Landmark Ed) **2022**; 27(12): 330
https://doi.org/10.31083/j.fbl2712330

Original Research

LncRNA *HIF1A-AS1* Regulates the Cellular Function of HUVECs by Globally Regulating mRNA and miRNA Expression

Zhiqiang Gong[1,†], Jin Yang[1,†], Junjie Dong[1], Haotian Li[1], Bing Wang[1], Kaili Du[1], Chunqiang Zhang[1], Lingqiang Chen[1,*]

[1]Department of Orthopaedics, The First Affiliated Hospital of Kunming Medical University, 650032 Kunming, Yunnan, China
*Correspondence: chenlqkm@sina.com (Lingqiang Chen)
[†]These authors contributed equally.
Academic Editor: Ioanna-Katerina Aggeli
Submitted: 8 September 2022 Revised: 1 November 2022 Accepted: 15 November 2022 Published: 21 December 2022

Abstract

Background: Long non-coding RNA (lncRNA) hypoxia inducible factor 1α-antisense RNA 1 (*HIF1A-AS1*) serves critical roles in cardiovascular diseases (CVDs). Vascular endothelial cells (VECs) are vulnerable to stimuli. Our previous study revealed that knockdown of *HIF1A-AS1* reduces palmitic acid-induced apoptosis and promotes the proliferation of human VECs (HUVECs); however, the underlying mechanism remains unclear. **Material and Methods**: Cell Counting Kit-8, flow cytometry, transwell invasion, and wound healing were applied to detect the function of HUVECs. Moreover, miRNA sequencing (miRNA-seq) and RNA sequencing (RNA-seq) were conducted to uncover its underlying mechanism. Quantitative Polymerase Chain Reaction (qPCR) was implemented to assess the accuracy of miRNA-seq. A co-expression network was generated to determine the relationship between differentially expressed miRNAs (DEmiRNAs) and differentially expressed genes (DEGs). **Results**: Knockdown of *HIF1A-AS1* promoted the proliferation, migration, and invasion but reduced the apoptosis of HUVECs, and the overexpression of this lncRNA had the opposite effect. Numerous DEmiRNAs and DEGs were identified, which might contribute to this phenomenon. Multiple target genes of DEmiRNAs were associated with cell proliferation and apoptosis, and overlapped with DEGs identified from RNA-seq. Finally, the network manifested that lncRNA *HIF1A-AS1* moderated the function of HUVECs by not only regulating the expression of some genes directly but also by influencing a few miRNAs to indirectly mediate the expression of mRNAs. **Conclusions**: The results suggested that *HIF1A-AS1* might regulate HUVEC function by not only regulating the expression of some genes directly but also by influencing some miRNAs to indirectly mediate the expression level of mRNA.

Keywords: *HIF1A-AS1*; HUVECs; miRNA; mRNA; cardiovascular diseases

1. Introduction

Cardiovascular disease (CVD) encompasses a variety of conditions that affect the heart and blood vessels, such as cerebrovascular disease, peripheral artery, and irregular heartbeat [1]. It is a serious threat to human health, characterized by a high prevalence, high disability rate, and high mortality. The number of people who die of CVD and cerebrovascular disease annually is up to 15 million, ranking first among all causes of death. Vascular endothelial cells (VECs), which are located in the innermost part of blood vessels, are vulnerable to stimuli. The apoptosis of VECs is closely correlated with numerous cardiovascular diseases (CVDs) such as arteriosclerosis, thrombus formation, and plaque erosion [2,3]. Due to the complex pathogenesis and serious complication, an increasing number of studies has focused on the etiology of VEC injury. However, the underlying mechanisms remains unclear, hindering the prevention and treatment of related diseases. Hence, it is necessary to identify novel apoptosis-related therapeutic targets in VECs for CVD.

In recent years, non-coding RNAs (ncRNAs), mainly circular RNAs, microRNAs (miRNAs), and long ncRNAs (lncRNAs), have been widely investigated [4]. LncRNA is widely expressed and plays an essential role in numerous life activities such as regulation of the cell cycle and cell differentiation. The abnormal expression or function of lncRNA is closely related to the occurrence of human diseases including cancer, immune responses, and other related diseases [5,6]. The biogenesis of lncRNA is associated with its specific subcellular localization and function. LncRNA is a potential biomarker that can be applied to clinical targeting and has potential therapeutic effects [7].

A number of noncoding RNAs, including lncRNAs and miRNAs, play pivotal roles in the progression of vascular diseases [8–12]. Some of them are emerging as diagnostic biomarkers or therapeutic targets due to their specific role in some CVDs [13–16]. LncRNA hypoxia inducible factor 1α-antisense RNA 1 (*HIF1A-AS1*), as one of three types of *HIF1A* antisense RNA, is located on the antisense strand of *HIF1A* of human chromosome 14, and its length is 652 nucleotides (nt) [17]. This lncRNA is widely distributed in the bone marrow, appendix, and gall bladder, among other organs. Furthermore, the expression of *HIF1A-AS1* shares a heterogeneous spatial distri-

Copyright: © 2022 The Author(s). Published by IMR Press.
This is an open access article under the CC BY 4.0 license.

Publisher's Note: IMR Press stays neutral with regard to jurisdictional claims in published maps and institutional affiliations.

bution across normal human tissues [18]. *HIF1A-AS1* is highly upregulated in human VECs (HUVECs) by acriflavine, a DNA topoisomerase inhibitor, which may also damage HUVECs [19]. Recent studies have demonstrated that this lncRNA might regulate the apoptosis and proliferation of vascular smooth muscle cells (VSMCs) [20]. In addition, *HIF1A-AS1* has pro-apoptotic and pro-inflammatory roles in Coxsackievirus B3-induced myocarditis by targeting miR-138 [21]. The interaction between apoptotic proteins and *HIF1A-AS1* plays an important role in the proliferation and apoptosis of VSMCs cultured *in vitro*, which might be involved in the pathogenesis of the thoracoabdominal aortic aneurysm [22]. *HIF1A-AS1* from exosomes could function as potential biomarkers for atherosclerosis [22]. Our previous studies indicated that the suppression of *HIF1A-AS1* can promote the proliferation and reduce the apoptosis of HUVECs induced by palmitic acid (PA) treatment [23], suggesting that this lncRNA might play critical roles in regulating HUVECs. However, the potential functions and regulatory mechanisms of this lncRNA in CVD related to HUVECs have not been fully elucidated. This study identifies novel therapeutic targets related to VEC apoptosis and provides new ideas for the treatment of CVDs, which is of great significance for the prevention and treatment of CVD.

In the current study, we elucidated the role of *HIF1A-AS1* in HUVECs and its underlying mechanisms. The results could provide insights into potential research directions for CVD treatment in the future. First, as previously reported [24], we simulated cardiovascular occlusion by treating HUVECs with PA. qPCR confirmed the successful transfection of plasmids containing *HIF1A-AS1* or short hairpin RNA (shRNA). Using flow cytometry, Cell Counting Kit-8 (CCK-8), transwell and wound healing assays, we found that this lncRNA promoted apoptosis and reduced proliferation, migration, and invasion. Moreover, miRNA sequencing (miRNA-seq) results showed that *HIF1A-AS1* globally mediated the expression of miRNAs. Bioinformatics analysis indicated that multiple target genes of differentially expressed miRNAs (DEmiRNAs) were involved in cell metabolism and apoptosis. Subsequently, RNA sequencing (RNA-seq) and bioinformatics analysis was applied to identify differentially expressed genes (DEGs). Interesting, quite a few DEGs overlapped with the target genes of DEmiRNAs. Finally, a co-expression network showed the strength of the correlation between expression levels of DEmiRNAs and some initial DEGs. These data suggest that *HIF1A-AS1* regulates the function of HUVECs by not only directly regulating the expression of some genes but also by influencing some miRNAs to indirectly mediate the expression of mRNA. The experimental process and relevant mechanism are schematically illustrated in Scheme.

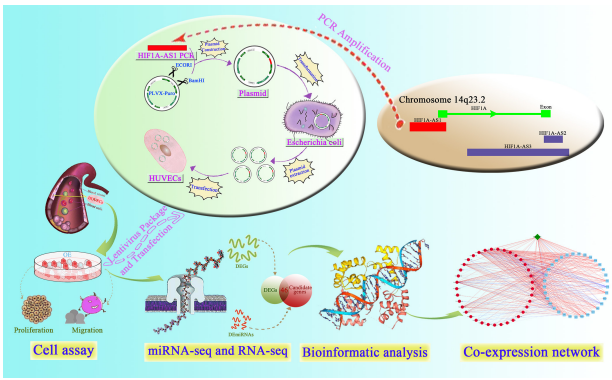

Scheme. Schematic of the experimental process and related mechanism.

2. Materials and Methods

2.1 Cell Culture

HUVECs were obtained from the Shanghai Cell Bank of the Chinese Academy of Sciences (Shanghai, China). The cells were taken from a male, and cells from passages 3 to 8 were used for the experiments. The cells were cultured in Dulbecco's modified Eagle medium (Catalog Number: 30030, Gibco, Waltham, MA, USA) containing 10% fetal bovine serum, 100 μg/mL streptomycin, and 100 U/mL penicillin. Then the cells were incubated at 37 °C in a standard atmosphere (Thermo Fisher Scientific, Waltham, MA, USA) with 5% CO_2.

2.2 Plasmid Generation, Lentivirus Package, and Transfection

HIF1-AS1 was amplified and subcloned into the EcoRI and BamHI restriction sites of pLVX-Puro 1.0 empty plasmid (Thermo Fisher Scientific). About 2 μg of plasmids was mixed with the lentivirus packaging plasmids pHelper 1.0, pHelper 2.0, and Opti-MEM according to a previous standard protocol [24]. Subsequently, the lentivirus was diluted in fresh medium and incubated for 24 h and the cells were washed. We silenced *HIF1A-AS1* in HUVECs using lentivirus-mediated shRNAs. The shRNAs targeting *HIF1A-AS1* were synthesized by Genepharm (Shanghai, China). Transfection of plasmids containing shRNAs or blank plasmids were conducted using Lipofectamine 3000 (Catalog Number: L3000001, Thermo Fisher Scientific, Shanghai, China) according to the manufacturer's protocol. The cloning primers and shRNAs are presented in Table 1.

2.3 Cell Proliferation Detection by the CCK-8 Assay

The proliferation of HUVECs was measured with the CCK-8 assay (Catalog Number: C0037, Beyotime, Shanghai, China). Briefly, HUVECs were cultured in 96-well plates for 24 h. The cells were divided into normal control (NC, untreated HUVECs), PA-treated HUVECs (PAT, 0.8 mmol/L), PAT + overexpression (OE) (*HIF1A-AS1* over-

Table 1. The primers used for qPCR and the shRNA sequences.

Gene/shRNA	Forward primer (5′-3′)	Reverse primer (5′-3′)
HIF1A-AS1	GCCTATGGTTGTTCATCTCGTCTC	TGCGTAAAGTACCGAAGAATGGAG
BAX	GATGATTGCCGCCGTGGAC	CCCAGTTGAAGTTGCCGTCAG
MMP1	GGGAGCAAACACATCTGACCTAC	AGTTGGAAGGCTTTCTCAATGGC
hsa-miR-1298-5p	ACACTCCAGCTGGGTTCATTCGGCTGTCCA	CTCAACTGGTGTCGTGGAGTCGGCAATTCAGTTGAGTACATCTG
hsa-miR-30c-5p	ACACTCCAGCTGGGTGTAAACATCCTACACT	CTCAACTGGTGTCGTGGAGTCGGCAATTCAGTTGAGGCTGAGAG
hsa-miR-27b-5p	ACACTCCAGCTGGGAGAGCTTAGCTGATTG	CTCAACTGGTGTCGTGGAGTCGGCAATTCAGTTGAGGTTCACCA
hsa-let-7a-5p	ACACTCCAGCTGGGTGAGGTAGTAGGTTGT	CTCAACTGGTGTCGTGGAGTCGGCAATTCAGTTGAGAACTATAC
hsa-miR-4664-3p	ACACTCCAGCTGGGCTTCCGGTCTGTGAGC	CTCAACTGGTGTCGTGGAGTCGGCAATTCAGTTGAGGACGGGGC
hsa-miR-769-5p	ACACTCCAGCTGGGTGAGACCTCTGGGTTC	CTCAACTGGTGTCGTGGAGTCGGCAATTCAGTTGAGAGCTCAGA
hsa-miR-106b-5p	ACACTCCAGCTGGGATCTGCACTGTCAGC	CTCAACTGGTGTCGTGGAGTCGGCAATTCAGTTGAGATCTGCAC
hsa-miR-548o-3p	ACACTCCAGCTGGGCCAAAACTGCAGTTA	CTCAACTGGTGTCGTGGAGTCGGCAATTCAGTTGAGGCAAAAGT
h-actin	TGGACTTCGAGCAAGAGATG	GAAGGAAGGCTGGAAGAGTG
U6	CTCGCTTCGGCAGCACA	AACGCTTCACGAATTGTGCGT
shRNA-1	ACCGGTGGGCATCCATAGACATATTCTTTCAAGAGAAGAATAATTGTCTATGGATGCCCTTTTTgaattc	
shRNA-2	ACCGGTGGAAACCTGAAACTTGAATGTTTCAAGAGAACATTCATAAGTTTCAGGTTTCCTTTTTgaattc	

expressed in PAT), PAT + sham-OE (PAT transfected with empty plasmid), PAT + sh (*HIF1A-AS1* knockdown in PAT), and PAT + sham-sh (PAT transfected with empty plasmid) groups. At 0, 24, 48, and 72 h, 10 μL CCK-8 reagent was added to each well, followed by incubation for 0.5 h. Finally, the absorbance was assessed at 450 nm with a microplate reader (Bio-Rad, Hercules, CA, USA, the number of version is 1681130A).

2.4 Flow Cytometry

The apoptosis of HUVECs was analyzed by flow cytometry using an Annexin V-Conjugated FITC Apoptosis Detection Kit (Catalog Number: BMS500FI-20, BD Biosciences, Franklin Lakes, NJ, USA). The cells were divided into NC, PAT, OE, sham-OE, sh, and sham-sh groups. Briefly, prepared cells were harvested after cultivating for 48 h, washed twice with phosphate-buffered saline (PBS) and incubated in the dark with Annexin V-FITC and propidium iodide (PI) for 30 min. Subsequently, the stained cells were detected with the MoFlo XDP flow cytometer (Catalog Number: V145577, Beckman, Brea, CA, USA) and Cell Quest 3.3 software (BD Biosciences).

2.5 Transwell Invasion

To perform the invasion assay, chambers were assembled in 24-well plates with 8 μM pore transwell inserts (Catalog Number: 353504, BD Falcon, Franklin Lakes, NJ, USA) coated with 50 μL Matrigel (diluted 1:4 in serum-free media). Treated cells (1×10^5) were added to the medium of the upper chamber. The invasive cells at the bottom of the implant were fixed in 4% paraformaldehyde and stained with 0.1% crystal violet. We captured images with a stereo microscope (Leica–M165 C, Wetzlar, Germany). Cell were counted under the TS100 microscope (Catalog Number: Eclipse TS100, Nikon Instruments, Shanghai, China).

2.6 Wound Healing

HUVECs (5×10^5 cells) were treated with the indicated drugs PA in a 6-well plate for 48 h. The next day, a 10 μL pipette tip was used to draw a linear or circular scratch wound in the confluent monolayer of cells. The cells were washed three times with PBS to remove the cell debris, and then cultured in fresh serum-free media for 12 h in 37 °C, 5% CO_2 incubator. Images of the wound were captured at 0, 24, and 48 h at 40× magnification, and ImageJ software (Mac v2.3.0, LOCI, University of Wisconsin, Madison, WI, USA) was used to measure the extent of the wound size in three wells per group.

2.7 RNA Extraction, Small RNA-seq and mRNA-seq

Total RNAs were extracted from HUVECs with TRIzol reagent (Catalog Number: 15596026, Invitrogen, Thermo Fisher Scientific). The absorbance of purified RNA at 260 and 280 nm and the A260:A280 ratio were measured using the NanoDrop ND-1000 spectrophotometer (Bio-Rad, Guangzhou, China). Six groups (NC, PAT, sham-OE, OE, sham-sh, and sh) were generated and two biological replicates were made.

Total RNAs (3 μg) from every sample were used to construct small RNA cDNA libraries with the Balancer NGS Library Preparation kit (Catalog Number: K02420-S, Gnomegen, San Diego, CA, USA). According to the manufacturer's protocol, the whole library was submitted to 10% native polyacrylamide gel electrophoresis. Then the corresponding strip into which miRNA was inserted was cut and eluted. These small RNA libraries were processed with NextSeq X-10 (Illumina, San Diego, CA, USA). The libraries were generated using purified mRNAs with the TruSeq Stranded Total RNA LT Sample Prep Kit (Catalog Number: RS-200-0012, Illumina, San Diego, CA, USA), according to the manufacturer's protocol. AMPure XP(Catalog Number: A63880, Beckman, USA) beads were

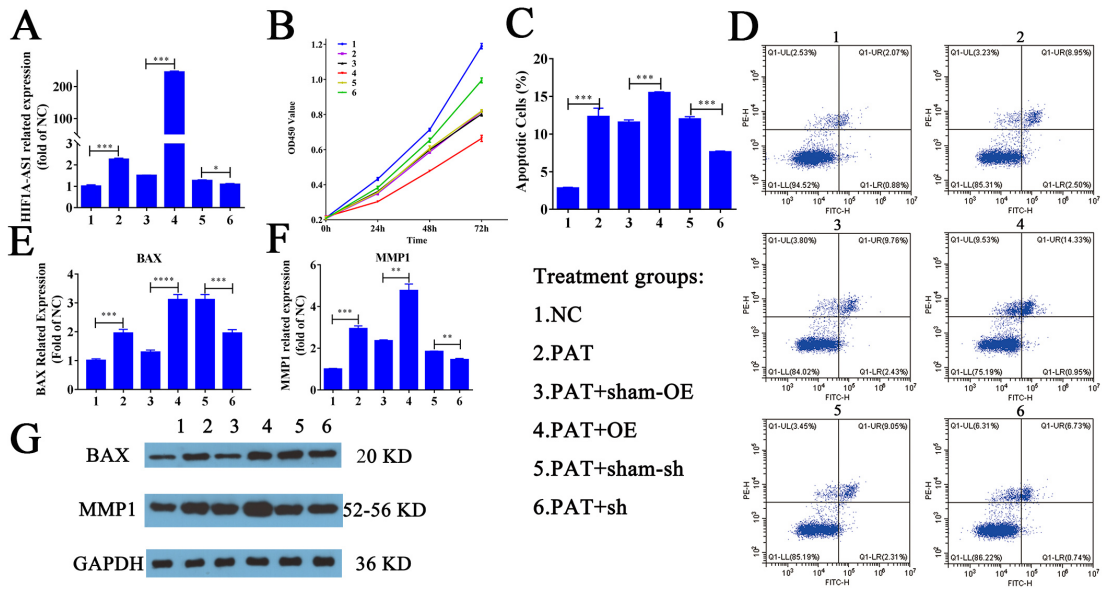

Fig. 1. Vector construction and *HIF1A-AS1* affects proliferation and apoptosis *in vitro*. (A) qPCR was used to verify the successful construction of the vector. (B) The CCK-8 assay was conducted to evaluate the cell proliferation of six treatment groups at 0, 24, and 48 h. The data are presented as the percentage relative to control cells and presented as the mean ± standard deviation (SD) of three replicates. (C) Apoptosis was detected using Annexin V-fluorescein isothiocyanate staining coupled with flow cytometry. Every group had three parallel controls. The upper left, upper right, and lower right quadrants represent necrotic, late apoptotic, and early apoptotic events, respectively. (D) Total percentage of apoptotic HUVECs in each treatment group were quantified with the data presented as the mean ± SD of three independent experiments. (E) qPCR was used to analyze expression of the pro-apoptotic protein *BAX*. (F) qPCR was conducted to detect the expression of migration-related protein *MMP1*. (G) WB was performed to assess the expression of *BAX* and *MMP1*. GAPDH was used as a loading control for WB. Statistical analysis was carried out using one-way ANOVA followed by Tukey's post hoc test. $*p < 0.05$, $**p < 0.005$, $***p < 0.001$, $****p < 0.0001$.

used to select cDNA with a length of 350 to 400 base pairs. To collect the RNA-seq data, the Nextseq X-10 system (Illumina, San Diego, CA, USA) was employed. RNA-seq data were mainly analyzed with Cytoscape (version 3.0.2, https://cytoscape.org/) and Hisat2 software (Hisat-2.1.0, The Johns Hopkins University, Baltimore, MD, USA).

2.8 Identification of Conserved and Novel miRNA

The FASTX-Toolkit (version 0.0.13, http://hannonlab.cshl.edu/fastx_toolkit/) was applied to process raw reads to obtain reliable clean reads. RNAs <18 or >35 nt in length were discarded from further analyses in view of the length of the mature miRNA and adapter lengths. Subsequently, the Rfam database (version 12.0, http://rfam.xfam.org/) was used to search the high-quality clean reads. Hereafter, the kept unique sequences were aligned against the miRBase database [25] by using Bowtie, with one mismatch allowed. The aligned small RNA sequences were matched by conserved miRNAs, and the unmatched sequences might be potential candidates for new miRNAs. Finally, the unique sequences were mapped to the reference genome sequence (GRCH38) of humans by the miRDeep algorithm to identify novel miRNAs [26].

2.9 qPCR

To validate the miRNA-seq data, qPCR was conducted. B-cell lymphoma 2 (Bcl-2)-associated X protein (*BAX*) and matrix metalloproteinase 1 (*MMP1*), key factors of HUVEC apoptosis and proliferation, were also validated by qPCR. The primers used are presented in Table 1. The PCR experiments were performed with the following conditions: pre-denaturation at 95 °C for 1 min, 40 cycles of denaturing at 95 °C for 15 s, annealing at 60 °C for 30 s, and elongation at 72 °C for 40 s. The results were calculated with the $2^{-\Delta\Delta Ct}$ method [27].

2.10 Western Blot Analysis

Western blotting (WB) was performed according to standard methods. Total cell lysates were made in 1× sodium dodecyl sulfate buffer. Equal protein concentrations were resolved by sodium dodecyl sulfate-polyacrylamide gel electrophoresis, and the proteins were electrotransferred to PVDF membranes (Bio-Rad). GAPDH (Sigma, St. Louis, MO, USA) was used as a loading control. Antibodies against *BAX* (1:2000) and *MMP1* (1:2000) were purchased from ProteinTech (*BAX* Catalog Number: 50599-2-Ig, *MMP1* Catalog Number: 10371-2-AP, Chicago, IL, USA).

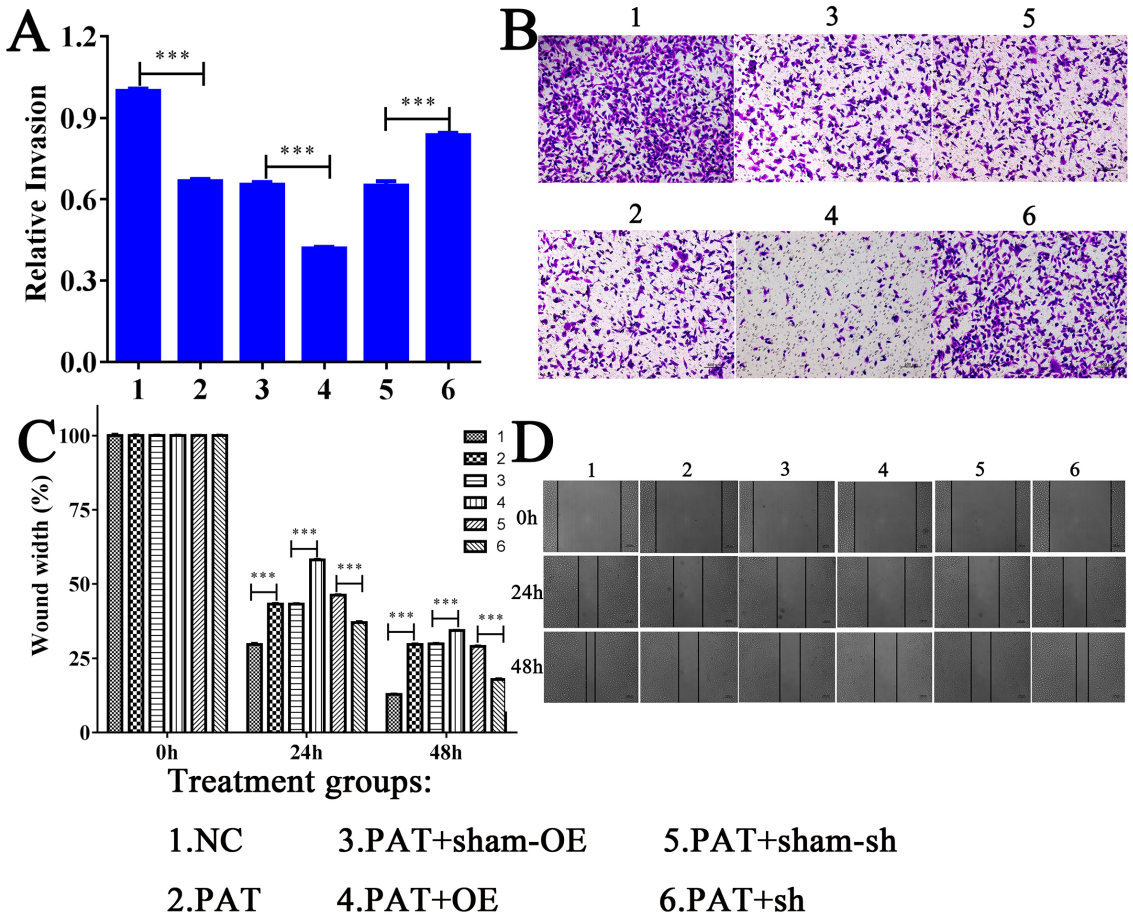

Fig. 2. *HIF1A-AS1* affects migration and invasion *in vitro*. (A) & (B) The wound healing assay was used to detect the relative cell migration in six groups of cells, scale bar = 200 μM. Quantitative analysis of wound healing was performed for three fields. The migration capability of *HIF1A-AS1* OE cells was significantly decreased. By contrast, *HIF1A-AS1* shRNA markedly enhanced cell migration compared to the sham-sh group. (C) & (D) The wound healing assay showed that *HIF1A-AS1* clearly decreased the invasion of the cells, whereas *HIF1A-AS1* silencing showed the opposite effect. The scale bar = 100 μM. The quantitative data of the transwell assay were obtained from five fields. Values shown are the mean $\pm$ SD from three independent experiments, $^{**}p < 0.005$, $^{***}p < 0.001$.

2.11 Bioinformatics Analysis

To detect the miRNA expression profile of the miRNAs identified, the frequencies of miRNA counts were normalized to transcripts per million (TPM) with the following formula: normalized expression = actual read count/total read count $\times$ 10^6. The strict standard of Padj <0.01 and $\log_2$ (fold change) >1 or $\log_2$ (fold change) <-1 indicated statistically significant DEmiRNAs. The expression profiles of mRNAs were normalized to fragments per kilobase of exon model per million mapped fragments. DEGs were obtained using the same method.

To predict the gene function of candidate genes or DEGs, Kyoto Encyclopedia of Genes and Genomes (KEGG) and Gene Ontology (GO) analyses were conducted using the DAVID bioinformatics database [28]. Co-expression networks were generated by calculating the Pearson's correlation coefficient (PCC) for the expression levels of candidate genes or DEGs. To display the co-expression networks, Cytoscape (version 3.0.2) was employed.

2.12 Statistical Analyses

All values are presented from independent experiments done in triplicate as the mean $\pm$ standard deviation. For comparison, GraphPad Prism 7 (GraphPad Software Inc., San Diego, CA, USA) was used, and the significance of differences between the means was determined by the Student's *t*-test or one-way analysis of variance. $p < 0.05$ was considered statistically significant result.

2.13 Online Data Deposition

The datasets generated in the current study were deposited in the Gene Expression Omnibus database of the National Center for Biotechnology Information under the accession numbers GSE107409 and GSE85610.

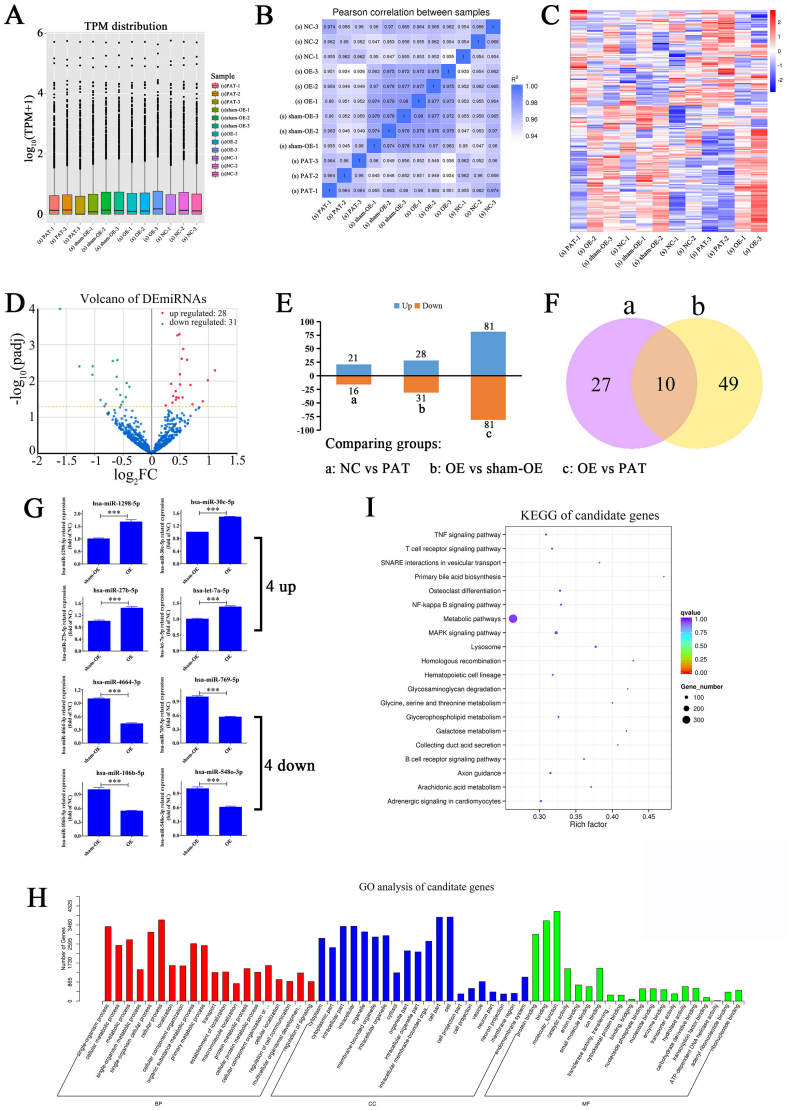

Fig. 3. Exploration of DEmiRNAs and functional analysis. (A) The boxplots of the 12 samples miRNAs, (s) stands for sample, n = 12. (B) OE of *HIF1A-AS1* could markedly regulate the expression of miRNAs. The results of Pearson's correlation data were presented. (C,D) Heat map (C) and Volcano plot (D) of DEmiRNAs expression profiles between OE and sham-OE. (E) The number of upregulated and downregulated DEmiRNAs among NC vs. PAT, OE vs. sham-OE, and OE vs. PAT. (F) Venn diagrams of the DEmiRNAs identified in different comparisons. Data are presented as the mean ± SD. (G) qPCR validation of certain DEmiRNAs identified by miRNA-sequencing in the OE and sham-OE groups. Statistical analysis was conducted by the Student's *t*-test, and data are presented as the mean ± SD and of experiments conducted in triplicate. (H,I) GO (H) and KEGG (I) pathway enrichment analyses of target genes from sham-OE vs. OE. DEmiRNAs, differentially expressed miRNAs; NC, normal control group; PAT, PA-treated HUVECs; PAT + sham-OE, HUVECs were treated with PA and then transfected with empty plasmid; PAT + OE, HUVECs were treated with PA and then transfected with *HIF1A-AS1* overexpressing plasmid; PAT + sham-sh, HUVECs were treated with PA and then transfected with empty plasmid; PAT + sh, HUVECs were treated with PA followed by knockdown of *HIF1A-AS1* with shRNA; qPCR, quantitative polymerase chain reaction. Upregulated miRNA: hsa-miR-1298-5p, hsa-miR-30c-5p, hsa-miR-27b-5p, hsa-let-7a-5p; downregulated miRNA: hsa-miR-4664-3p, hsa-miR-769-5p, hsa-miR-106b-5p, hsa-miR-548o-3p. ***$p < 0.001$.

3. Results

3.1 LncRNA HIF1A-AS1 Regulates the Proliferation of HUVECs

We constructed a model of cardiovascular occlusion by treating HUVECs with PA [23]. To investigate how *HIF1A-AS1* regulates HUVEC function, we overexpressed or knocked down this lncRNA in PA-treated HUVECs (Fig. 1A), and analyzed its expression level by qPCR (**Supplementary Figs. 1,2**). Compared with the NC group, the overexpression and knockdown of *HIF1A-AS1* were

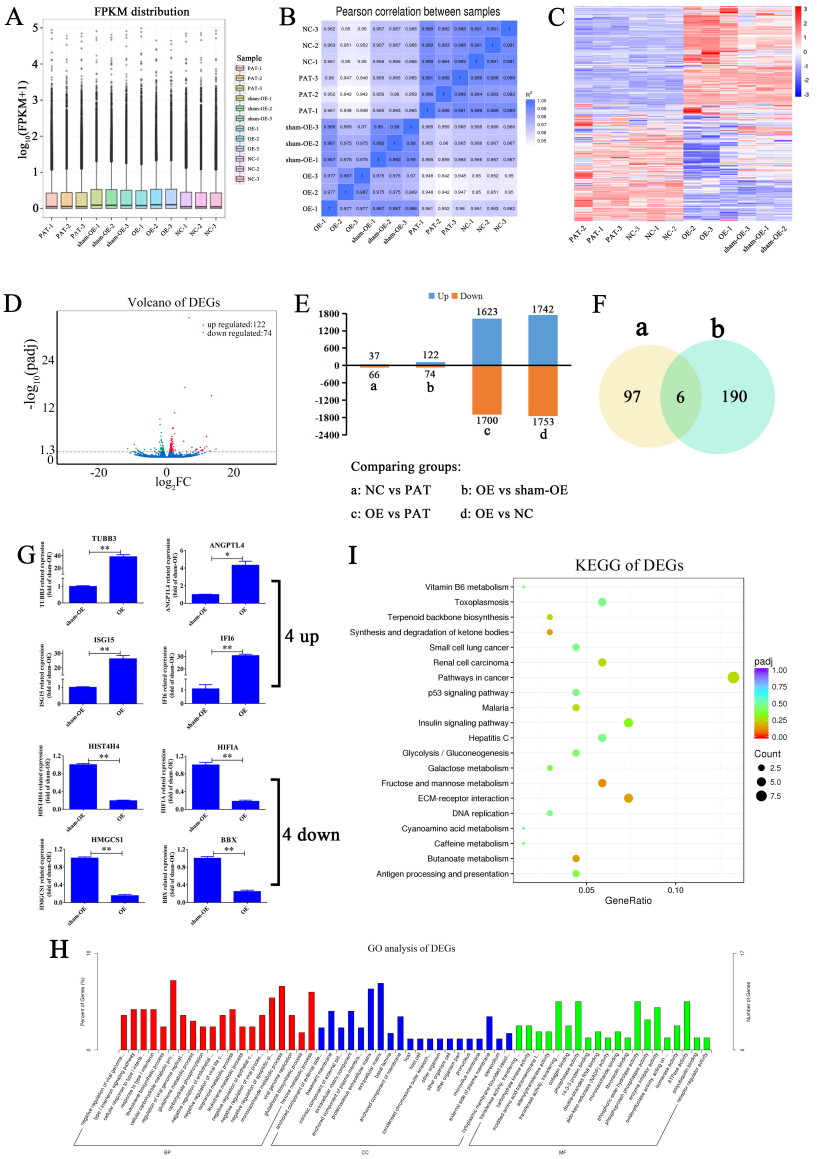

Fig. 4. Exploration of DEGs and functional analysis. (A) Boxplots of the 12 samples RNA-seq; no significant difference was found among these groups. (B) Subsequently, the RNA-seq results revealed that OE of *HIF1A-AS1* not only regulate the expression of miRNAs but also genes. (C,D) Heat map (C) and Volcano plot (D) of DEGs expression profiles between the OE and sham-OE groups. (E) The number of upregulated and down-regulated DEGs among NC vs. PAT, OE vs. sham-OE and OE vs. PAT groups. (F) Venn diagrams of the DEGs identified in different comparisons. Data are presented as the mean ± SD. (G) qPCR were carried out for validation of certain DEGs identified by mRNA-seq in the OE and sham-OE groups. Statistical analysis was conducted by the Student's *t*-test and data are presented as the mean ± SD and experiment was performed in triplicate. (H,I) GO (H) and KEGG (I) pathway enrichment analyses of DEGs from sham-OE vs. OE. DEGs, differently expressed genes. Up-regulated mRNA: *TUBB3*, *ANGPTL4*, *ISG15*, *IFI6*; down-regulated mRNA: *HIST4H4*, *HIF1A*, *HMGCS1*, *BBX*. *$p < 0.05$, **$p < 0.01$.

successful. Then, we obtained six groups of cells with different treatment strategies, namely NC, PAT, PAT + sham-OE, PAT + OE, PAT + sham-sh, and PAT + sh groups.

The effect of *HIF1A-AS1* on the proliferation of HUVECs was determined with a CCK-8 kit. A significant time-dependent increase in proliferation was found among the six groups. CCK-8 assays showed that treatment of HUVECs with PA for 72 h resulted in a 45.8% reduction in HUVEC survival. Silencing of *HIF1A-AS1* significantly increased the absorbance values at all time points (24, 48, 72 h). In addition, OE of *HIF1A-AS1* led to a 17.1% reduction of its basal inactivation (45.8%) at 72 h (Fig. 1B). The results of the CCK-8 assay indicated that silencing of *HIF1A-AS1* promoted the proliferation of HUVECs, and OE led to the reverse effect.

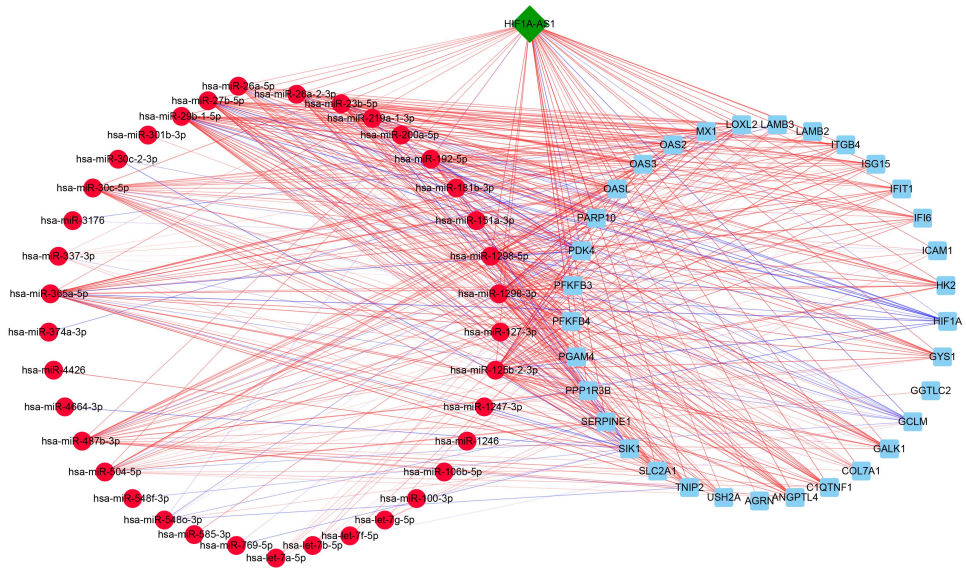

Fig. 5. Interaction network analysis of DEmiRNAs and DEGs associated with some important pathways. Network analysis on the basis of PCCs for DEmiRNAs and DEGs enriched in 'negative regulation of endothelial cell apoptotic process' (GO:2000352), 'cellular carbohydrate metabolic process' (GO:0044262), 'type I interferon signaling pathway' (GO:0060337) and so on. Circular nodes represent DEmiRNAs and rectangular nodes signify DEGs, while these solid lines represent significant correlations between DEmiRNAs and DEGs. The red lines represent negative correlation, while the blue lines represent positive correlation. $p < 0.01$ and PPC ≥ 0.06 indicated a statistically significant correlation. PCC, Pearson's correlation coefficient; miRNA, microRNA.

Flow cytometry was conducted to count the number of apoptotic cells. After treatment of HUVECs with PA, the number of apoptotic cells increased more than 3 times (Fig. 1C). Indeed, the apoptosis of HUVECs has been identified as a crucial factor in the pathogenesis of various CVD processes [29,30]. Thus, preventing the apoptosis of HUVECs may be a novel strategy for the treatment of CVD. Fig. 1C shows that silencing *HIF1A-AS1* led to about 35.5% recovery, and OE led to 28.5% promotion of basal apoptosis induced by PA. These results suggest that the lncRNA *HIF1A-AS1* plays a critical role in regulating the apoptosis and proliferation of HUVECs.

The expression of *BAX* and *MMP1*, key regulators of HUVEC apoptosis and proliferation, was analyzed by qPCR (Fig. 1E,F) and WB (Fig. 1G and **Supplementary Figs. 3,4,5**). Quantitative analysis of the WB results was also performed (**Supplementary Fig. 6**), which was consistent with the corresponding qPCR results. Compared with the sham-OE group, the expression of *BAX* and *MMP1* was significantly increased in the OE group. These data indicate that OE of this lncRNA promotes PA-induced apoptosis and reduces the proliferation of HUVECs.

3.2 LncRNA HIF1A-AS1 Regulates the Migration and Invasion of HUVECs

The transwell migration assay was performed to determine whether OE of *HIF1A-AS1* can mediate the migration and invasion of HUVECs. In this assay, the cell invasion ability of PA-treated HUVECs decreased about 49.8% compared with blank groups. A 27.8% recovery was observed in invading cells upon silencing of *HIF1A-AS1* compared to sham-sh cells, suggesting that silencing this lncRNA can enhance the migration ability of HUVECs. Conversely, OE of *HIF1A-AS1* resulted in another 35.3% reduction, clearly indicating the weakened migratory ability of PA-treated HUVECs (Fig. 2A,B).

To further estimate the migration effect of *HIF1A-AS1* lncRNA on HUVECs, we conducted a wound healing assay. As shown in Fig. 2C,D, the migration ability was weakened after OE of *HIF1A-AS1* compared with the sham-OE group. By contrast, HUVECs migrated for a longer distance in the pore plate extracted from *HIF1A-AS1* transgenic cells than from the sham-sh group. These results suggested that this lncRNA successfully inhibited HUVEC migration.

3.3 LncRNA HIF1A-AS1 Globally Regulates the Expression of miRNAs

To investigate how *HIF1A-AS1* regulates the expression of miRNAs in HUVECs, 12 small RNA libraries (NC-1, NC-2, NC-3, PAT-1; PAT-2, PAT-3, PAT-sham-OE-1, PAT-sham-OE-2; PAT-sham-OE-3, PAT-OE-1, PAT-OE-2 and PAT-OE-3) were constructed for miRNA-seq. More than 141.2 million reads were generated, with approximately 11.8 million sequence reads per sample. Comparing all reads to the human reference genome, it was found that 91.2% of the reads were successfully mapped to the reference genome (Table 2). More than 852 conserved miRNAs and about 29 novel miRNAs were identified from the

Table 2. Small RNA-seq results.

Sample name	Raw reads	Clean reads	Total sRNA	Mapped sRNA	Conserved miRNA	Novel miRNA
NC-1	10396456	10095959	10174904	8663662	630	13
NC-2	12281806	12148322	9880267	9134235	756	22
NC-3	12371135	12173628	9043012	8697259	796	23
PAT-1	12063104	11945895	10223291	9580570	763	20
PAT-2	11548214	11351509	14008342	12347805	747	20
PAT-3	9967884	9844849	10032489	9188302	674	19
PAT-sham-OE-1	11524964	11310117	10449928	9418015	854	29
PAT-sham-OE-2	12595778	12406547	10637694	9785800	888	26
PAT-sham-OE-3	15271004	15102718	13704766	12264356	920	31
PAT-OE-1	10825192	10686483	9844659	8803245	812	25
PAT-OE-2	10901089	10702730	9502391	8298306	792	25
PAT-OE-3	11455474	11268048	8817627	8188634	856	27

boxplots of the 12 samples, no obvious differences were found in these groups (Fig. 3A and **Supplementary Table 1**). The above results confirmed the reliability and stability of miRNA-seq.

3.4 Identification of DEmiRNAs

MiRNAs act as key post-transcriptional regulators in multiple cellular biological processes such as proliferation, differentiation, apoptosis, invasion and migration [31]. Interestingly, we found that OE of *HIF1A-AS1* markedly regulated the expression of miRNAs. The results of the Pearson correlation data are shown in Fig. 3B. A heat map was generated to reflect the detailed alterations of miRNAs (Fig. 3C). In addition, the volcano plots in Fig. 3D compared these $\log_2$ fold change values with their respective p ($-\log_{10}$) values to obtain the distributions of both upregulated and downregulated DEmiRNAs. By setting a strict threshold, a total of 59 statistically significant DEmiRNAs were identified in the OE vs. sham-OE group (Fig. 3E and **Supplementary Table 2**). Furthermore, the Venn diagram showed 10 reliable core miRNAs across two groups between PAT vs. NC and OE vs. sham-OE (Fig. 3F). These findings indicate that *HIF1A-AS1* is associated with the expression levels of some miRNAs in HUVECs. To confirm the accuracy and reliability of the miRNA assays, the expression levels of certain DEmiRNAs, including four upregulated miRNAs (hsa-miR-1298-5p, hsa-miR-30c-5p, hsa-miR-27b-5 and hsa-let-7a-5p) and four downregulated miRNAs (hsa-miR-4664-3p, hsa-miR-769-5p, hsa-miR-106b-5p and hsa-miR-548o-3p), were further validated by qPCR. All of the miRNAs were randomly selected from those 59 DEmiRNAs. The primers used are presented in Table 1. The results were in accordance with the miRNA-seq results (Fig. 3G).

3.5 Target Genes of DEmiRNA Are Mainly Related to Apoptosis and Metabolism

MiRNAs commonly exert their functions through binding to complementary target sites from the target genes. DEmiRNA was obtained from OE vs. sham-OE groups. The DEmiRNA target genes, also called candidate genes, were successively identified by miRBase. As shown in **Supplementary Table 3**, we obtained a total of 2030 and 2401 predicted targets of the upregulated and downregulated DEmiRNAs, respectively. For the 28 upregulated DEmiRNAs, hsa-miR-193b-3p was found to potentially target the most genes, with a number of 334. For the 31 downregulated DEmiRNAs, hsa-miR-5088-5p possessed the most targets, with a number of 1087.

It was obvious that OE of *HIF1A-AS1* globally affected miRNA expression in HUVECs. Consequently, bioinformatics analysis was conducted to identify the key functions in which all candidate genes were involved. GO analysis showed that target genes were mainly enriched in the single-organism process (GO:0044699), cellular process (GO:0009987), and some metabolic processes, especially the organic substance metabolic process (GO:0071704). Furthermore, cellular component analysis indicated that the target genes were mainly enriched in the intracellular regions and shared a heterogeneous spatial distribution across the entire cell. In addition, molecular function analysis showed that most of them performed binding activities and enzymatic reactions (Fig. 3H).

KEGG enrichment analysis of the target genes was performed to gain further insight into their functions (**Supplementary Table 4**). The results showed that most of the candidate genes were enriched in pathways associated with metabolism including metabolic pathways (ID: hsa01100), glycerophospholipid metabolism (ID: hsa00564), glycosaminoglycan degradation (ID: hsa00531), galactose metabolism (ID: hsa00052), hematopoietic cell lineage (ID: hsa04640), and glycine, serine, and threonine metabolism (ID: hsa00260) (Fig. 3I). It can be proved from the previous discussion that *HIF1A-AS1* overexpression in HUVECs can produce numerous complex changes, indicating that it plays an important role in CVD.

Table 3. mRNA-seq results.

Sample name	Raw reads	Clean reads	Total mapped	Multiple mapped	Uniquely mapped
NC-1	92950742	90845448	85500273	3714836	81785437
NC-2	88259194	86224692	81248247	4094785	77153462
NC-3	96525162	94188860	88406416	4294222	84112194
PAT-1	101172612	98776918	92458131	4556970	87901161
PAT-2	106123908	102950612	95273281	6263675	89009606
PAT-3	105586716	102833318	95759913	5149250	90610663
sham-OE-1	101559260	99046714	90953710	4024188	86929522
sham-OE-2	103669156	101555434	91930479	4509528	87420951
sham-OE-3	101384686	99407612	90783970	4071846	86712124
OE-1	105385816	103382496	88847622	4617749	84229873
OE-2	99645746	95951214	84091509	5573479	78518030
OE-3	102004516	97888796	86382747	5694658	80688089

3.6 mRNA Expression Profiles and Their Bioinformatics Analysis

RNA-seq experiments were done to further explore the molecular mechanisms by which *HIF1A-AS1* regulates HUVECs. More than 1.20 billion pairend reads were generated, corresponding with ~100 million sequence reads per sample. Using Hisat2 software, >85.9% of clean reads were successfully mapped against the current human reference genome (GRCH38). The ratio of multiple mapped reads was less than 6.1% (Table 3). There was no significant difference among these groups in the boxplots (Fig. 4A).

Subsequently, the RNA-seq results revealed that OE of *HIF1A-AS1* regulated the expression for both miRNA and mRNA. Pearson's correlation data are shown in Fig. 4B. The heat map reflected the DEGs (Fig. 4C). By adopting the same method, a total of 196 DEGs were obtained from the sham-OE vs. OE groups (**Supplementary Table 5**), with 122 upregulated and 74 downregulated, respectively (Fig. 4D,E). We observed six reliable core mRNAs across two groups (PAT vs. NC and OE vs. sham-OE) from the Venn diagram (Fig. 4F). qPCR was conducted to verify the four upregulated mRNAs (*TUBB3*, *ANGPTL4*, *ISG15* and *IFI6*) and four downregulated mRNAs (*HIST4H4*, *HIF1A*, *HMGCS1* and *BBX*) (Fig. 4G). The qPCR results were in accordance with that of mRNA-seq. Interestingly, 23.5% DEGs overlapped with DEmiRNA target genes. The overlapping DEGs are listed in **Supplementary Table 6**. According to previous reports [27–29], both mRNA and miRNAs had the ability to regulate the apoptosis and proliferation of HUVECs. To further explore the role of miRNA in HUVECs, we conducted this study.

Since some DEGs overlapped with DEmiRNA target genes, bioinformatics analysis was conducted to identify the biological function of DEGs. GO enrichment analysis showed that most of the enriched pathways were associated with multiple metabolic process, signaling pathways, and apoptosis with high confidence. Remarkably, the outcome also highlighted large-scale alterations in a variety of metabolic pathways and apoptosis processes upon the elevation of *HIF1A-AS1* levels. Similarly, the results also demonstrated that a larger number of DEGs were related to extracellular matrices with overlapping distributions, and others were restricted to particular cellular loci. The majority had binding functions and enzymatic activity, especially transferase activity, with a fraction of them having other housekeeping functions (Fig. 4H and **Supplementary Table 7**).

The most significantly enriched KEGG pathways are shown in Fig. 4I and **Supplementary Table 8**. The results showed that fructose and mannose metabolism (ID: hsa00051), synthesis and degradation of ketone bodies (ID: hsa00072) and butanoate metabolism (ID: hsa00650) were the most significant pathways for enrichment. KEGG results showed that some DEGs were more uniformly enriched in tumor-related pathways such as p53 signaling pathway (ID: hsa04115), renal cell carcinoma (ID: hsa05211), Vitamin B6 metabolism (ID: hsa00750), pathways in cancer (ID: hsa05200), malaria (ID: hsa05144), and caffeine metabolism (ID: hsa00232). The main signaling and metabolism pathways determined by KEGG analysis will provide further insight into future research directions on mRNA.

3.7 Integrative Analysis of DEmiRNA and mRNA Expression

Generally, miRNAs have the capacity to recognize and bind to complementary 3'-untranslated regions of target mRNAs, which can lead to the degradation or transcriptional repression of mRNAs [32]. To explore the relationship between DEmiRNA and DEGs, a co-expression network was generated by calculating the PCC for the expression levels of DEGs and DEmiRNAs. It showed a close correlation between the expression levels of DEmiRNAs and DEGs, which were enriched in some initial pathways (Fig. 5). A total of 37 DEmiRNAs and 33 DEGs were filtered into the co-expression network complex. The network manifested that lncRNA *HIF1A-AS1* mediated the function

of HUVECs by not only regulating the expression of some genes directly but also influencing a few miRNAs to indirectly mediate the expression level of mRNA. These findings may explain the underlying mechanism of *HIF1A-AS1* in CVD.

4. Discussion

Most CVDs are related to the apoptosis of VECs, which is the main form of vascular injury [33]. Previous studies have shown that the broken balance between VECs apoptosis and proliferation markedly contributes to the pathogenesis of CVD [23,34]. An increasing number of studies has shown the critical effect of lncRNAs on regulating the proliferation and apoptosis of VECs in CVD [3,35,36].

Only about 2% of sequences in the human genome possess the ability of encoding proteins. Accumulating evidence has revealed that lncRNAs are related to human diseases as a biomarker or therapeutic target [37,38]. Postnatally, lncRNAs have attracted a lot of attention due to their variety of biological roles including cell cycle control, cell proliferation, apoptosis, transwell invasion, embryonic development, and carcinogenesis by mediating the gene expression at the transcriptional, splicing, transportation, and translational levels [39,40].

MiRNAs involved in mRNA degradation or translation inhibition [41] are a group of evolutionarily conserved ncRNAs about 20–22 nt in length from hairpin pre-miRNA precursors [42]. Accumulative evidence has revealed that miRNAs, alone or in combination with lncRNAs, are involved in regulating specific gene expression at the translation or transcription level. Then they can alter cell signaling pathways associated with different physiological and pathological processes [43–46].

A study found that *HIF1A-AS1* TFR2 forms triplexes with EPH receptor A2 (EPHA2) and adriamycin (ADM) double-stranded DNA under regular and triplex-stabilized conditions upon DNA hairpin formation. Increasing the expression of HIF1A-AS1 can inhibit the expression of EPHA2 and ADM, whereas the downregulation of *HIF1A-AS1* produces opposite results. These results suggest that the trimer formation region can mediate EPHA2 and ADM inhibition [47]. Another study showed that the *HIF1A-AS1* was significantly increased in gemcitabine (GEM)-resistant pancreatic cancer cells. *HIF1A-AS1* enhanced the GEM resistance of pancreatic cancer cells by upregulating the expression of HIF1α and promoting glycolysis. *HIF1A-AS1* may be a new therapeutic target for GEM resistance of pancreatic cancer in the future [48]. In our study, we overexpressed or knocked down this lncRNA in PA-treated HUVECs to explore how *HIF1A-AS1* efficiently regulates the function of HUVECs.

Another study, which was published recently, showed that some lncRNAs regulate various cellular processes by acting as competing endogenous RNAs (ceRNAs) and binding proteins. For example, *HIF1A-AS1*, acting as a ceRNA, absorbed miR-204 to evaluate Suppressor of Cytokine Signaling 2 expression in cardiac function [21]. This lncRNA participates in the regulation of proliferation, apoptosis, and the activity of the extracellular matrix proteins of VSMCs [18,49]. Abundant evidence has indicated that this lncRNA might participate in the development of CVD by regulating the PA-induced apoptosis of HUVECs [23]. However, the molecular mechanism by which *HIF1A-AS1* interacts with miRNAs and mRNA and their regulatory roles of pathogenesis are unclear. *HIF1A-AS1* has potential as a novel therapeutic target in CVD, but underlying information about the regulatory mechanisms in HUVECs is lacking.

It is known that miRNAs are involved in the progression and pathogenesis of VECs [50]. In this study, it was found that OE of *HIF1A-AS1* reduced the cellular growth rate and led to the robust apoptosis of HUVECs. We further studied the molecular mechanism of this phenomenon using miRNA-seq and RNA-seq. More than 852 conserved miRNAs were identified and about 29 novel miRNAs were found by miRNA-seq in the sham-OE group. When *HIF1A-AS1* was overexpressed, the expression levels of some miRNAs markedly changed, indicating that this lncRNA may play a critical role in miRNA-based therapies. The target genes of those DEmiRNAs were successively predicted by miRase. Additionally, multiple target genes of the DEmiRNAs were associated with the apoptosis, proliferation, and migration of HUVECs, suggesting that OE of *HIF1A-AS1* could inhibit proliferation and promote the apoptosis of HUVECs by mediating miRNA expression. As previously reported, lipids have important functions in maintaining normal physiological cellular functions [51]. Glycosaminoglycan can promote wound healing. The administration of d-galactose to animals decreases the proliferation of cells and reduces the migration and survival of new neurons in the granule cell layer [52]. Researchers have found a potential involvement of the glycine-serine-threonine metabolic axis in longevity and related molecular mechanisms [53]. Thus, DEmiRNA may serve a regulatory role in the molecular functional analysis of HUVECs.

Subsequently, RNA-seq was performed to identify the DEGs. Cluster of differentiation, which leads to endothelium apoptosis, was not identified. Individual differences may be responsible for this unusual phenomenon. Many DEGs were found to overlap with the target genes of DEmiRNA. Furthermore, both mRNA and miRNAs could regulate the apoptosis and proliferation of HUVECs [54–56]. Therefore, *HIF1A-AS1* has the ability to regulate the expression of some miRNAs, which could target some apoptosis-related genes by degrading mRNAs or inhibiting their translation. The crosstalk among miRNAs, lncRNAs, and mRNA shows a complex network of gene expression regulation [57]. Hence, in the present study, a co-expression network was systematically constructed

to explore the relationship among lncRNA *HIF1A-AS1*, DEmiRNA, and DEGs. The findings revealed that the expression levels of the DEmiRNAs was tightly linked to the apoptosis-related DEGs. However, this network has not been systematically validated, which limits the comprehensive understanding of the mechanisms underlying the role of *HIF1a-AS1* in the treatment of CVD. In addition, accumulative evidence has indicated that *ANGPTL4* is directly correlated with the risk of CVD, especially atherosclerosis [58]. *SERPINE1* may serve as a potential therapeutic target or new biomarkers in acute myocardial infarction [59]. Interferon Alpha Inducible Protein 6, which is a mitochondrial localized antiapoptotic protein, contributes to promoting the metastatic potential of certain cancer cells through mitochondrial reactive oxygen species [60]. However, in this co-expression network, the expression levels of these CVD-related genes were tightly related to certain miRNAs. Therefore, *HIF1A-AS1* can modulate the expression of DEGs by mediating miRNA expression. The present study reveals a novel mechanism by which *HIF1A-AS1* regulates the apoptosis of HUVECs.

5. Conclusions

In summary, our study showed that *HIF1A-AS1* regulated HUVEC function by not only regulating the expression of some genes directly but also influencing some miRNAs to indirectly mediate the expression level of mRNA, indicating that it may play a key role in the pathogenesis and progression of CVD. The current study also provides some new insights and directions for the prevention and treatment of CVD. Although the clinical applications need to be further explored, these results additionally provide insight into the molecular mechanisms by which *HIF1A-AS1* affects HUVECs and a scientific experimental basis for treating CVD. Thus, it is feasible that the co-expression network could be applied for the prevention, diagnosis, treatment, and prognosis of CVD. However, further studies are being conducted to more systematically elucidate the role of *HIF1A-AS1* in CVD and further determine the potential clinical role of the co-expression network.

Availability of Data and Materials

The datasets analyzed in this study can be obtained from the NCBI public repository under accession numbers GSE107409 and GSE85610.

Author Contributions

ZG, JY designed and managed the project. JD, HL, BW, KD drafted the manuscript. CZ, LC participated in sample collection and manuscript revision. All authors read and approved the final manuscript.

Ethics Approval and Consent to Participate

Not applicable.

Acknowledgment

Not applicable.

Funding

This study was supported by National Natural Science Foundation of China (NSFC) (Grant Nos.: 81860093 and 81660215) and Associated Project of Yunnan Province Science & Technology Department and Kunming Medical University Basic Research for Application [Grant Nos.: 202101AY070001-031, 2019FE001(-207), and 202101AT070226].

Conflict of Interest

The authors declare no conflict of interest.

Supplementary Material

Supplementary material associated with this article can be found, in the online version, at https://doi.org/10.31083/j.fbl2712330.

References

[1] Park JH, Dehaini D, Zhou J, Holay M, Fang RH, Zhang L. Biomimetic nanoparticle technology for cardiovascular disease detection and treatment. Nanoscale Horizons. 2020; 5: 25–42.

[2] Marziano C, Genet G, Hirschi KK. Vascular endothelial cell specification in health and disease. Angiogenesis. 2021; 24: 213–236.

[3] Lu W, Huang SY, Su L, Zhao BX, Miao JY. Long Noncoding RNA LOC100129973 Suppresses Apoptosis by Targeting miR-4707-5p and miR-4767 in Vascular Endothelial Cells. Scientific Reports. 2016; 6: 21620.

[4] Zhang C, Niu K, Lian P, Hu Y, Shuai Z, Gao S, *et al*. Pathological Bases and Clinical Application of Long Noncoding RNAs in Cardiovascular Diseases. Hypertension. 2021; 78: 16–29.

[5] Coelho-Lima J, Spyridopoulos I. Non-coding RNA regulation of T cell biology: Implications for age-associated cardiovascular diseases. Experimental Gerontology. 2018; 109: 38–46.

[6] Poller W, Dimmeler S, Heymans S, Zeller T, Haas J, Karakas M, *et al*. Non-coding RNAs in cardiovascular diseases: diagnostic and therapeutic perspectives. European Heart Journal. 2018; 39: 2704–2716.

[7] Statello L, Guo CJ, Chen LL, Huarte M. Gene regulation by long non-coding RNAs and its biological functions. Nature Reviews Molecular Cell Biology. 2021; 22: 96–118.

[8] Zhao X, Su L, He X, Zhao B, Miao J. Long noncoding RNA CA7-4 promotes autophagy and apoptosis via sponging MIR877-3P and MIR5680 in high glucose-induced vascular endothelial cells. Autophagy. 2020; 16: 70–85.

[9] Luo Y, Fang Z, Ling Y, Luo W. LncRNA-H19 acts as a ceRNA to regulate HE4 expression by sponging miR-140 in human umbilical vein endothelial cells under hyperglycemia with or without α-Mangostin. Biomedicine and Pharmacotherapy. 2019; 118: 109256.

[10] Zhang JR, Sun HJ. MiRNAs, lncRNAs, and circular RNAs as mediators in hypertension-related vascular smooth muscle cell dysfunction. Hypertension Research. 2021; 44: 129–146.

[11] Kumar S, Williams D, Sur S, Wang JY, Jo H. Role of flow-sensitive microRNAs and long noncoding RNAs in vascular dysfunction and atherosclerosis. Vascular Pharmacology. 2019; 114: 76–92.

[12] Indolfi C, Iaconetti C, Gareri C, Polimeni A, De Rosa S. Non-coding RNAs in vascular remodeling and restenosis. Vascular Pharmacology. 2019; 114: 49–63.
[13] Simion V, Haemmig S, Feinberg MW. LncRNAs in vascular biology and disease. Vascular Pharmacology. 2019; 114: 145–156.
[14] Jaé N, Heumüller AW, Fouani Y, Dimmeler S. Long non-coding RNAs in vascular biology and disease. Vascular Pharmacology. 2019; 114: 13–22.
[15] Fasolo F, Di Gregoli K, Maegdefessel L, Johnson JL. Non-coding RNAs in cardiovascular cell biology and atherosclerosis. Cardiovascular Research. 2019; 115: 1732–1756.
[16] Kumar MM, Goyal R. LncRNA as a Therapeutic Target for Angiogenesis. Current Topics in Medicinal Chemistry. 2017; 17: 1750–1757.
[17] Wang YK, Liu CM, Lin T, Fang CY, Yu CC, Yu CH. Inhibition of HIF1A-AS1 impedes the arecoline-induced migration activity of human oral mucosal fibroblasts. Journal of the Formosan Medical Association. 2020; 119: 879–883.
[18] Xu J, Zhang Y, Chu L, Chen W, Du Y, Gu J. Long non-coding RNA HIF1A-AS1 is upregulated in intracranial aneurysms and participates in the regulation of proliferation of vascular smooth muscle cells by upregulating TGF-β1. Experimental and Therapeutic Medicine. 2019; 17: 1797–1801.
[19] Seredinski S, Boos F, Günther S, Oo JA, Warwick T, Izquierdo Ponce J, *et al*. DNA topoisomerase inhibition with the HIF inhibitor acriflavine promotes transcription of lncRNAs in endothelial cells. Molecular Therapy - Nucleic Acids. 2022; 27: 1023–1035.
[20] Wang S, Zhang X, Yuan Y, Tan M, Zhang L, Xue X, *et al*. BRG1 expression is increased in thoracic aortic aneurysms and regulates proliferation and apoptosis of vascular smooth muscle cells through the long non-coding RNA HIF1A-AS1 in vitro. European Journal of Cardio-Thoracic Surgery. 2015; 47: 439–446.
[21] Cao H, Yang B, Zhao Y, Deng X, Shen X. The pro-apoptosis and pro-inflammation role of LncRNA HIF1A-AS1 in Coxsackievirus B3-induced myocarditis via targeting miR-138. Cardiovascular Diagnosis and Therapy. 2020; 10: 1245–1255.
[22] Wang Y, Liang J, Xu J, Wang X, Zhang X, Wang W, *et al*. Circulating exosomes and exosomal lncRNA HIF1A-AS1 in atherosclerosis. International Journal of Clinical and Experimental Pathology. 2017; 10: 8383–8388.
[23] Wang J, Chen L, Li H, Yang J, Gong Z, Wang B, *et al*. Clopidogrel reduces apoptosis and promotes proliferation of human vascular endothelial cells induced by palmitic acid via suppression of the long non-coding RNA HIF1A-AS1 in vitro. Molecular and Cellular Biochemistry. 2015; 404: 203–210.
[24] Cribbs AP, Kennedy A, Gregory B, Brennan FM. Simplified production and concentration of lentiviral vectors to achieve high transduction in primary human T cells. BMC Biotechnology. 2013; 13: 98.
[25] Kozomara A, Griffiths-Jones S. miRBase: annotating high confidence microRNAs using deep sequencing data. Nucleic Acids Research. 2014; 42: D68–D73.
[26] Friedländer MR, Chen W, Adamidi C, Maaskola J, Einspanier R, Knespel S, *et al*. Discovering microRNAs from deep sequencing data using miRDeep. Nature Biotechnology. 2008; 26: 407–415.
[27] Livak KJ, Schmittgen TD. Analysis of relative gene expression data using real-time quantitative PCR and the 2(-Delta Delta C(T)) Method. Methods. 2001; 25: 402–408.
[28] Huang da W, Sherman BT, Lempicki RA. Systematic and integrative analysis of large gene lists using DAVID bioinformatics resources. Nature Protocols. 2009; 4: 44–57.
[29] Izumi Y, Kim S, Yoshiyama M, Izumiya Y, Yoshida K, Matsuzawa A, *et al*. Activation of apoptosis signal-regulating kinase 1 in injured artery and its critical role in neointimal hyperplasia. Circulation. 2003; 108: 2812–2818.
[30] Yamada S, Ding Y, Tanimoto A, Wang KY, Guo X, Li Z, *et al*. Apoptosis signal-regulating kinase 1 deficiency accelerates hyperlipidemia-induced atheromatous plaques via suppression of macrophage apoptosis. Arteriosclerosis, Thrombosis, and Vascular Biology. 2011; 31: 1555–1564.
[31] Giovannetti E, Erozenci A, Smit J, Danesi R, Peters GJ. Molecular mechanisms underlying the role of microRNAs (miRNAs) in anticancer drug resistance and implications for clinical practice. Critical Reviews in Oncology/Hematology. 2012; 81: 103–122.
[32] Lv M, Zhong Z, Huang M, Tian Q, Jiang R, Chen J. lncRNA H19 regulates epithelial-mesenchymal transition and metastasis of bladder cancer by miR-29b-3p as competing endogenous RNA. Biochimica et Biophysica Acta-Molecular Cell Research. 2017; 1864: 1887–1899.
[33] Pestana CR, Urbaczek AC, Alberici JV, Rodrigues GJ, Carrilho E. Metabolic profiling of human endothelial cells during autophagy assessed in a biomimetic microfluidic device model. Life Sciences. 2017; 172: 42–47.
[34] Mauro M, Zlatopolskiy A, Raife TJ, Laurence J. Thienopyridine-linked thrombotic microangiopathy: association with endothelial cell apoptosis and activation of MAP kinase signalling cascades. British Journal of Haematology. 2004; 124: 200–210.
[35] Zhang BY, Jin Z, Zhao Z. Long intergenic noncoding RNA 00305 sponges miR-136 to regulate the hypoxia induced apoptosis of vascular endothelial cells. Biomedicine and Pharmacotherapy. 2017; 94: 238–243.
[36] Lu W, He X, Su L, Zhao B, Miao J. Effects of annexin A7 inhibitor-ABO on the expression and distribution of long noncoding RNA-CERNA1 in vascular endothelial cells apoptosis. Apoptosis. 2019; 24: 552–561.
[37] Okazaki Y, Furuno M, Kasukawa T, Adachi J, Bono H, Kondo S, *et al*. Analysis of the mouse transcriptome based on functional annotation of 60,770 full-length cDNAs. Nature. 2002; 420: 563–573.
[38] Kapranov P, Cheng J, Dike S, Nix DA, Duttagupta R, Willingham AT, *et al*. RNA maps reveal new RNA classes and a possible function for pervasive transcription. Science. 2007; 316: 1484–1488.
[39] Mercer TR, Dinger ME, Mattick JS. Long non-coding RNAs: insights into functions. Nature Reviews Genetics. 2009; 10: 155–159.
[40] Fatica A, Bozzoni I. Long non-coding RNAs: new players in cell differentiation and development. Nature Reviews Genetics. 2014; 15: 7–21.
[41] Bartel DP. MicroRNAs: target recognition and regulatory functions. Cell. 2009; 136: 215–233.
[42] Bartel DP. MicroRNAs: genomics, biogenesis, mechanism, and function. Cell. 2004; 116: 281–297.
[43] Nemecz M, Alexandru N, Tanko G, Georgescu A. Role of MicroRNA in Endothelial Dysfunction and Hypertension. Current Hypertension Reports. 2016; 18: 87.
[44] Zhang Y, Sun X, Icli B, Feinberg MW. Emerging Roles for MicroRNAs in Diabetic Microvascular Disease: Novel Targets for Therapy. Endocrine Reviews. 2017; 38: 145–168.
[45] Chen HS, Tong HS, Zhao Y, Hong CY, Bin JP, Su L. Differential Expression Pattern of Exosome Long Non-Coding RNAs (lncRNAs) and MicroRNAs (miRNAs) in Vascular Endothelial Cells Under Heat Stroke. Medical Science Monitor. 2018; 24: 7965–7974.
[46] Zhang Y, Liu X, Bai X, Lin Y, Li Z, Fu J, *et al*. Melatonin prevents endothelial cell pyroptosis via regulation of long noncoding RNA MEG3/miR-223/NLRP3 axis. Journal of Pineal Research. 2018; 64: e12449.
[47] Leisegang MS, Bains JK, Seredinski S, Oo JA, Krause NM, Kuo

CC, *et al*. HIF1α-AS1 is a DNA:DNA:RNA triplex-forming lncRNA interacting with the HUSH complex. Nature Communications. 2022; 13: 6563.
[48] Xu F, Huang M, Chen Q, Niu Y, Hu Y, Hu P, *et al*. LncRNA HIF1A-AS1 Promotes Gemcitabine Resistance of Pancreatic Cancer by Enhancing Glycolysis through Modulating the AKT/YB1/HIF1α Pathway. Cancer Research. 2021; 81: 5678–5691.
[49] Zhang X, Li H, Guo X, Hu J, Li B. Long Noncoding RNA Hypoxia-Inducible Factor-1 Alpha-Antisense RNA 1 Regulates Vascular Smooth Muscle Cells to Promote the Development of Thoracic Aortic Aneurysm by Modulating Apoptotic Protease-Activating Factor 1 and Targeting let-7g. The Journal of Surgical Research. 2020; 255: 602–611.
[50] Yamakuchi M. MicroRNAs in Vascular Biology. International Journal of Vascular Medicine. 2012; 2012: 794898.
[51] Zeng C, Wen B, Hou G, Lei L, Mei Z, Jia X, *et al*. Lipidomics profiling reveals the role of glycerophospholipid metabolism in psoriasis. GigaScience. 2017; 6: 1–11.
[52] Sun Y, Shi H, Yin S, Ji C, Zhang X, Zhang B, *et al*. Human Mesenchymal Stem Cell Derived Exosomes Alleviate Type 2 Diabetes Mellitus by Reversing Peripheral Insulin Resistance and Relieving β-Cell Destruction. ACS Nano. 2018; 12: 7613–7628.
[53] Aon MA, Bernier M, Mitchell SJ, Di Germanio C, Mattison JA, Ehrlich MR, *et al*. Untangling Determinants of Enhanced Health and Lifespan through a Multi-omics Approach in Mice. Cell Metabolism. 2020; 32: 100–116.e4.
[54] Wu X, Zheng X, Cheng J, Zhang K, Ma C. LncRNA TUG1 regulates proliferation and apoptosis by regulating miR-148b/IGF2 axis in ox-LDL-stimulated VSMC and HUVEC. Life Sciences. 2020; 243: 117287.
[55] Li L, Wang M, Mei Z, Cao W, Yang Y, Wang Y, *et al*. lncRNAs HIF1A-AS2 facilitates the up-regulation of HIF-1α by sponging to miR-153-3p, whereby promoting angiogenesis in HUVECs in hypoxia. Biomedicine and Pharmacotherapy. 2017; 96: 165–172.
[56] Hao X, Li Q, Guo J, Ren X, Feng Y, Shi C, *et al*. Multifunctional Gene Carriers with Enhanced Specific Penetration and Nucleus Accumulation to Promote Neovascularization of HUVECs in Vivo. ACS Applied Materials & Interfaces. 2017; 9: 35613–35627.
[57] Tay Y, Rinn J, Pandolfi PP. The multilayered complexity of ceRNA crosstalk and competition. Nature. 2014; 505: 344–352.
[58] Aryal B, Price NL, Suarez Y, Fernández-Hernando C. ANGPTL4 in Metabolic and Cardiovascular Disease. Trends in Molecular Medicine. 2019; 25: 723–734.
[59] Chen DQ, Kong XS, Shen XB, Huang MZ, Zheng JP, Sun J, *et al*. Identification of Differentially Expressed Genes and Signaling Pathways in Acute Myocardial Infarction Based on Integrated Bioinformatics Analysis. Cardiovascular Therapeutics. 2019; 2019: 8490707.
[60] Cheriyath V, Kaur J, Davenport A, Khalel A, Chowdhury N, Gaddipati L. G1P3 (IFI6), a mitochondrial localised antiapoptotic protein, promotes metastatic potential of breast cancer cells through mtROS. British Journal of Cancer. 2018; 119: 52–64.